# Modification of deposition process for Cu(In, Ga)$Se_2$ thin film solar cells on polyimide substrate at low temperature*

**XIN Zhi-jun** (辛治军)[1]**, **CHEN Xi-ming** (陈希明)[1]**, **QIAO Zai-xiang** (乔在祥)[2], **WANG He** (王赫)[2], **XUE Yu-ming** (薛玉明)[1], **PAN Zhen** (潘振)[2], **and TIAN Yuan** (田园)[3]

*1. Tianjin Key Laboratory of Film Electronic & Communication Devices, School of Electronics Information Engineering, Tianjin University of Technology, Tianjin 300384, China*

*2. National Key Laboratory of Power Sources, Tianjin Institute of Power Sources, Tianjin 300381, China*

*3. School of Mater. Sci. & Eng., Hebei University of Technology, Tianjin 300130, China*

(Received 27 August 2012)



We fabricate polycrystalline Cu(In, Ga)$Se_2$ (CIGS) film solar cells on polyimide (PI) substrate at temperature of 450 °C with single-stage process, and obtain a poor crystallization of CIGS films with several secondary phases in it. For improving it further, the two-stage process is adopted instead of the single-stage one. An extra Cu-rich CIGS layer with the thickness from 100 nm to 200 nm is grown on the substrate, and then another Cu-poor CIGS film with thickness of 1.5−2.0 μm is deposited on it. With the modification of the evaporation process, the grain size of absorber layer is increased, and the additional secondary phases almost disappear. Accordingly, the overall device performance is improved, and the conversion efficiency is enhanced by about 20%.

**Document code:** A **Article ID:** 1673-1905(2013)02-0112-4

**DOI** 10.1007/s11801-013-2340-z

Cu(In, Ga)$Se_2$ (CIGS) solar cells have demonstrated a very high efficiency of 20.3% on glass substrate[1]. Recently, solar cells on flexible substrate have drawn more and more attention, because they can be fabricated by using roll-to-roll deposition process with very high throughput[2]. Additionally, the flexible substrates offer the advantages for monolithically interconnected module development. However, the CIGS absorber layer is usually deposited around 480 °C[3], and the influence of coefficient of thermal expansion (CTE) becomes a critical problem at this temperature[4]. In this paper, CIGS absorber layers are deposited on flexible polyimide (PI) substrate at 450 °C. Deposition process is optimized by adding an extra Cu-rich step before depositing CIGS absorber layer to improve the quality of crystallization of the CIGS film, and the properties of films and devices are investigated.

Devices were prepared on 50 μm-thick PI films, and an approximate 600 nm-thick Mo bilayer was deposited by direct current (DC) sputtering as the back contact. The CIGS absorber layer with thickness of 1.5−2.0 μm was deposited in high vacuum environment with single-stage and two-stage processes, respectively. Both processes started with the deposition of a $(In_{1-x}Ga_x)_2Se_3$ (IGS) precursor layer (200 nm-thick) at 350 °C, 10 nm NaF was deposited on the precursor, and then the substrate temperature was increased to 450 °C. In the single-stage process, the four elements were co-evaporated on NaF layer. In the two-stage process, firstly a thin Cu layer was deposited on NaF layer, which makes the layer fully Cu-rich, and then the four elements were co-evaporated with decreasing the Cu evaporation rate slightly. Se was evaporated throughout the whole layer growth in constant overpressure. In the final CIGS films, Cu/(Ga + In) is in the range of 0.80−0.90, and Ga/(Ga + In) is in the range of 0.25−0.30. Subsequently, the CIGS films were covered by an approximate 70 nm-thick CdS layer grown with a chemical bath deposition (CBD) method. A 50 nm-thick high-resistance intrinsic-ZnO (i-ZnO) and 500 nm-thick high-conductivity ZnO:Al bilayer were deposited by a radio frequency (RF) sputtering as the front contact window layer[5]. The Ni/Al (30 nm/2 μm) grid was deposited by electron beam evaporation to complete the device. No anti-reflection coatings were applied, and the cell with the area of 0.2 $cm^2$ approximately was isolated by mechanically scribing.

The general deposition temperature for high quality CIGS film is 500 °C approximately or even high during the evaporation process. For two types of commercial available PI substrates of Kapton and Upiles, the CTEs

* This work has been supported by the National High Technology Research and Development Program of China (No. 2012AA050701).

** E-mails: xinzhijun0218@163.com; xmchen2006@126.com

of CIGS films are very different at such a substrate temperature[4]. Because of the mismatch of CTEs between PI, Mo and CIGS layers, CIGS film cracks or even peels off. Poor adhesion can cause more electricity leakage channels, and it is the most serious problem of the CIGS solar cells on flexible PI substrate[5].

On the other hand, typically high efficiency CIGS thin film solar cells require to incorporate 0.01%−0.1%[8] sodium (Na) into the CIGS absorber layers. It is very important for improving the properties of CIGS films and the performance of solar cells on the substrates without sodium, like PI foils. Sodium can be incorporated into CIGS absorber layers during various stages of film growth with compounds or elemental Na[9]. In this paper, 10 nm-thick NaF was deposited prior to the CIGS layer. It can affect the contact between Mo and CIGS layers. The CIGS film can peel off with slight curve after finishing the CIGS film. To avoid this, we deposit 200 nm-thick IGS precursor before NaF deposition to improve the CTE matching of this multi-layer structure.

In the new two-stage process, we only co-evaporate Cu and Se on the IGS precursor for a short time ($\Delta t$) about 2−4 min, making the layer fully Cu-rich. However, if $\Delta t$ is too long, the Cu element will react with the IGS compound and the by-products will diffuse to the bottom of absorber layer. Thus, the role of IGS layers on improving the adhesion between the CIGS and Mo films can be traded off, and it causes serious degradation of the electrical and structural properties of CIGS film.

The surface and cross-section SEM images of CIGS films grown at different deposition processes are shown in Fig.1. The quality of crystallization of CIGS film deposited by the two-stage process is improved greatly. The surfaces of CIGS films for both deposition processes are smooth and with many triangle grains as shown in Fig.1(a) and (b), respectively. It is attributed to the composition of Cu/(In+Ga)<0.90[10,11]. However, the grain size of CIGS film deposited by the single-stage process is smaller, and numerous tiny grains distribute among the larger grains. Fig.1(c) and (d) show the cross-section images of two samples. It is found that the grains of CIGS absorber layer for both processes are compact and lathy. Fig.1(d) shows that the grain size of the film deposited by the two-stage process is larger, growing almost from the Mo layer to the top of absorber layer, and there is no weeny grain at the bottom of CIGS film. Co-evaporation of Cu and Se elements onto IGS precursor layer makes the film fully Cu-rich, which assists the grains and the film in growing and recrystallizing[12]. As a result, the grain size of CIGS film increases, and the number of small grains near the Mo back contact decreases obviously.

The structural properties of CIGS films deposited by the two processes are investigated by XRD. As shown in Fig.2, the XRD spectra of CIGS films from different processes exhibit strong peaks of (112) and (220)/(204), and the preferential orientation of grains is (112) in the layer. However, the obvious difference is that there is an additional peak of secondary phase $(In, Ga)_2Se_3$ at $2\theta$= 25.5°, as shown in Fig.2(a). The existence of $(In, Ga)_2Se_3$ phases can be attributed to the incomplete diffusion reaction between the metal elements and selenium due to the limited heat energy from the substrate at lower temperature[13,14].

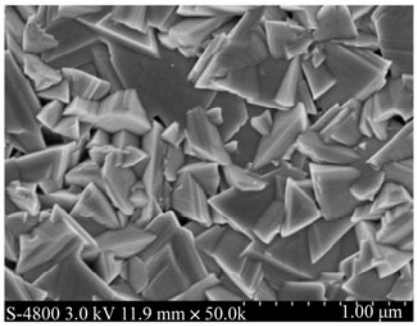


(a) Surface in the single-stage process

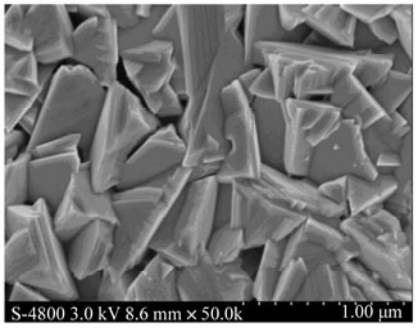


(b) Surface in the two-stage process

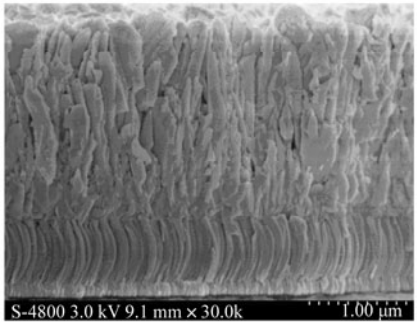


(c) Cross-section in the single-stage process

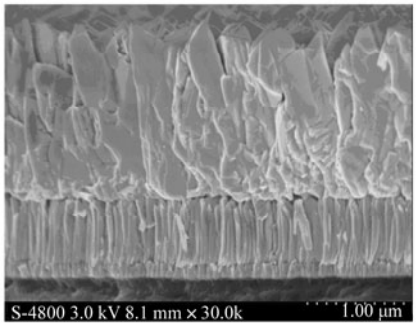


(d) Cross-section in the two-stage process

**Fig.1 Surface and cross-sectional images of CIGS films deposited by different processes**

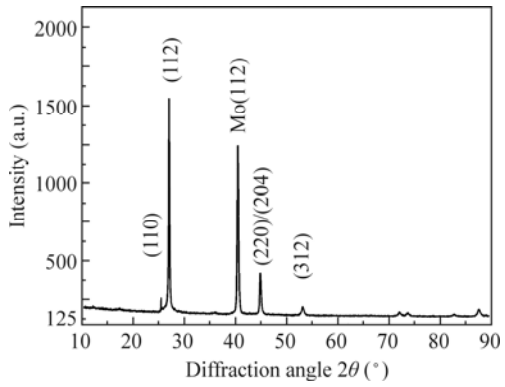


(a) Single-stage process

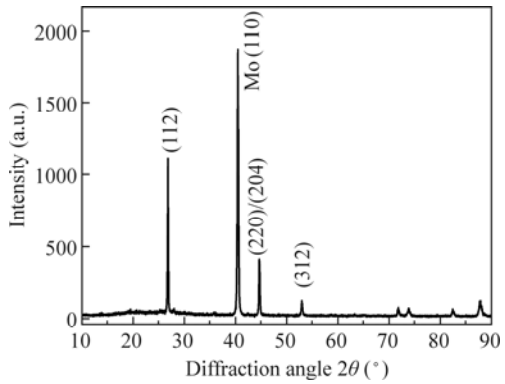


(b) Two-stage process

**Fig.2 XRD spectra of CIGS films with different deposition processes**

The Raman measurements help to discern the structure of the CIGS film surfaces. As shown in Fig.3, the Raman spectra present the expected values for the main chalcopyrite A1 peak around 176 $cm^{-1}$ and the mixed modes between 200 $cm^{-1}$ and 250 $cm^{-1}$[15]. However, there is a distinct peak at 260 $cm^{-1}$ for the single-stage process. It can be concluded that a possible presence of the Cu-rich phase, i.e., $Cu_xSe$, exists on/near the surface of absorber layer[16]. It is mainly attributed to the different reaction paths of the growing absorber layers for different deposition processes.

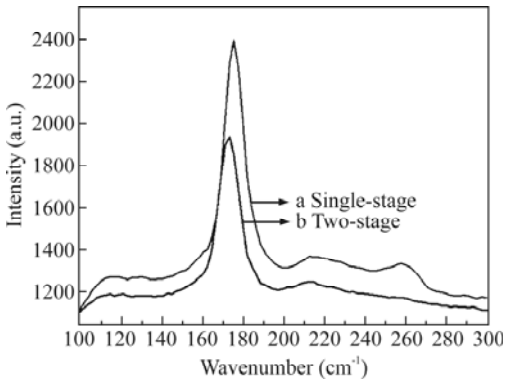


**Fig.3 Raman spectra of CIGS absorber with different deposition processes**

In single-stage process, four elements of Cu, In, Ga and Se are co-evaporated with a constant rate at lower temperature of 450 °C. The metal elements may be combined with selenium to form CIGS quaternary phase directly or to form binary selenides firstly, i.e., In-Se, Ga-Se and Cu-Se, and then they react with each other to produce CIGS phase. The obvious defect of this process is that the evaporation rate of Cu is lower than that of In and Ga all the time, resulting in Cu-poor film during the growth of CIGS film. This can be affected by the reaction rate among the four elements or binary phases, especially at lower substrate temperature, because the elements and compounds can not get enough thermal energy for the inter-diffusion and combination. As a result, the additional secondary phases shown in Figs.1 and 2 exist in the bulk or on the surface of the film.

However, at the beginning of the two-stage process, Cu and Se atoms are deposited onto IGS precursor layer firstly, producing Cu-rich film. Followed by evaporating Cu, In and Ga elements on the substrate, they react with the Cu-rich phase to form CIGS quaternary phase with a slight Cu-poor composition ultimately. It can be assumed that CIGS film is grown through a Cu-rich process, the Cu-rich CIGS layer has significantly different compositions in the bulk and on the surface, leading to a stoichiometric large chalcopyrite grain[17-19], and then the Cu-poor CIGS is continuously deposited, which grows along the large grains. Although the deposition temperature in this paper is 450 °C, which is lower than the liquid phase temperature of $Cu_xSe$, the grain size, especially at the bottom of CIGS film, is larger than that of single-step process obviously. It is also supported by the model based on grain boundary migration, and argues that a liquid Cu-Se phase is not a necessary precondition for the achievement of CIGS layers with large grains, which is proposed by Barreau[20].

The performance of CIGS solar cells deposited with different processes is investigated by external quantum efficiency (EQE) and *J-V* measurements as shown in Figs.4 and 5, respectively. Fig.4 shows the response intensities of the solar cells are low for both two processes, which can be enhanced by adding an anti-reflection layer to reduce the reflection loss. Almost similar EQEs are obtained for wavelength region up to 500 nm. The EQE of the two-stage process device increases slightly in the wavelength region from 500 nm to 1000 nm. It can be attributed to the improvement of the absorption and collection of photo-induced carriers in CIGS film, resulting in higher $J_{sc}$ as shown in Fig.5. It can be found that the photovoltaic (PV) performance is improved significantly by using the modified process. The conversion efficiency is increased from 6.78% to 8.11%. The modified deposition process improves the quality of crystallization of the CIGS solar cell, which results in the reduction of defect state density and conductivity compared with the single-stage process, and thus reduces the recombination of the photo-induced carriers, which leads to enhanced $J_{sc}$ from 24.46 mA/$cm^2$ to 26.43 mA/$cm^2$, $V_{oc}$ from 520.4 mV to 535.6 mV and *FF* from 53.3% to 57.3%. The PV parameters for both devices are limited by relatively low deposition temperature[14].

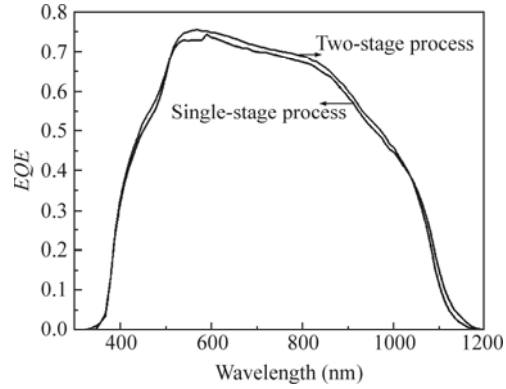


**Fig.4 EQE curves of CIGS solar cells using different deposition processes**

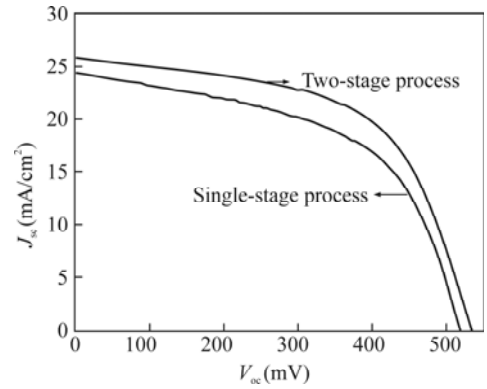


**Fig.5 *J-V* curves of the two devices using different deposition processes**

The CIGS solar cells are fabricated at relatively low substrate temperature of 450 °C. The influence of the two co-evaporation processes on the crystal quality and the device performance is investigated. It can be seen that the Cu-rich CIGS deposited after the IGS precursor is vital for improving the device performance. The new deposition process results in large grain size, and it is confirmed that it is necessary to pass through a Cu-rich composition during the deposition process[19]. A conversion efficiency of 8.11% is achieved with the reduction of recombination losses caused by the grain boundaries. A further enhancement can be realized by optimizing the co-evaporation process, controlling the amount of sodium, adjusting deposition time $\Delta t$, and finding the suitable precursor with little influence on device performance.

**Acknowledgements**

We thank the CIGS teams at CETC.

## References

[1] P. Jackson, D. Hariskos, E. Lotter, S. Paetel, R. Wuerz, R. Menner, W. Wischmann and M. Powalla, Progress in Photovoltaics: Research and Applications **19**, 894 (2011).

[2] J. R. Tuttle, A. Szalaj and J. A. Keane, 15.2% AMO/1433 W/kg Thin Film CIGS Solar Cell for Space Applications, Conference Record of the 28th IEEE Photovoltaic Specialists Conference, 1042 (2000).

[3] Adrian Chirila, Stephan Buecheler, Fabian Pianezzi, Patrick Bloesch, Christina Gretener, Alexander R. Uhl, Carolin Fella, Lukas Kranz, Julian Perrenoud, Sieghard Seyrling, Rajneesh Verma, Shiro Nishiwaki, Yaroslav E. Romanyuk, Gerhard Bilger and Ayodhya N. Tiwari, Nature Materials **10**, 857 (2011).

[4] LI Bo-yan, ZHANG Yi, LIU Wei and SUN Yun, Optoelectronics Letters **8**, 348 (2012).

[5] H. Wang, Y. Zhang, X. L. Kou, Y. A. Cai, W. Liu, T. Yu, J. B. Pang, C. J. Li and Y Sun, Semicond. Sci. Technol. **25**, 055007 (2010).

[6] Friedrich Kesslera and Dominik Rudmann, Solar Energy **77**, 685 (2004).

[7] JIANG Wei-long, HE Qing, LIU Wei, YU Tao, LIU Fang-fang, PANG Jin-bo, LI Feng-yan, LI Chang-jian and SUN Yun, Journal of Optoelectronics· Laser **21**, 1657 (2010). (in Chinese)

[8] A. Rockett, J. S. Britt, T. Gillespie, C. Marshall, M. M. Al Jassim, F. Hasoon, R. Matson and B. Basol, Thin Solid Films **372**, 212 (2000).

[9] D. Rudmann, G. Bilger, M. Kaelin, F. J. Haug, H. Zogg and A. N. Tiwari, Thin Solid Films **431**, 37 (2003).

[10] Zhang L., Researches on Depositing CIGS Thin Films at Low Substrate Temperature and the Performance of CIGS Solar Cells with Polyimide Substrate, PhD. Thesis Institute of Photoelectron Thin-Film Device and Technology, Nankai University, Tianjin, China (2008).

[11] J. Scholdstrom, J. Kessler and M. Edoff, Thin Solid Films **480**, 61 (2005).

[12] S. Seyrling, A. Chirila, D. Guttler, P. Blosch, F. Pianezzi, R. Verma, S. Bucheler, S. Nishiwaki, Y. E. Romanyuk, P. Rossbach and A. N. Tiwari, Solar Energy Materials & Solor Cells **95**, 1477 (2011).

[13] A. M. Gabor, J. R. Tuttle, M. H. Bode, A. Franz, A. L. Tennant, M. A. Contreas, R. Noufi, D. G. Jensen and A. M. Hermann, Materials and Solar Cells **41-42**, 247 (1996).

[14] S. R. Kodigala, Thin Films and Nanostructures **35**, 123 (2010).

[15] Xu C. M., Xu X. L., Xu J., Yang X. J., Zuo J., Kong N., Huang W. H. and Liu H. T., Semicond. Sci. Technol. **19**, 1201 (2004).

[16] R. Caballero, C. Kaufmann, A. V. Efimova, T. Rissom, V. Hoffmann and H. W. Schock, Investigation of Cu(In, Ga)$Se_2$ Thin-film Formation during the Multi-stage Co-evaporation Process, Prop. Photovolt: Res. Appl., 1233 (2012).

[17] R. Caballero, V. Izquierdo-Roca, X. Fontane, C. A. Kaufmann, J. Alvarez-Garcia, A. Eicke, L. Calvo-Barrio, A. Perez-Rodriguze, H. K. Schock and J. R. Morante, Acta Materialia **58**, 3468 (2010).

[18] J. Kessler, C. Chityuttakan, J. Lu, J. Scholdstrom and L. Stolt, Prog. Photovolt: Res. Appl. **11**, 319 (2003).

[19] J. Kessler, C. Chityuttakan, J. Scholdstrom and L. Stolt, Thin Solid Films **431-432**, 1 (2003).

[20] N. Barreau, T. Painchaud, F. Couzinie-Devy, L. Arzel and J. Kessler, Acta Materialia **58**, 5572 (2010).